Electrochemically Controllable Growth and Tunable Optical Properties of Zn1−xCdxO Alloy Nanostructures

ARTICLE *in* CRYSTAL GROWTH & DESIGN · MARCH 2009

Impact Factor: 4.89 · DOI: 10.1021/cg800496d

5 AUTHORS, INCLUDING:

Yexiang Tong
Sun Yat-Sen University
297 PUBLICATIONS **8,173** CITATIONS

SEE PROFILE

Electrochemistry Communications 11 (2009) 282–285

Contents lists available at ScienceDirect

Electrochemistry Communications

journal homepage: www.elsevier.com/locate/elecom

A novel electrochemical deposition route for the preparation of $Zn_{1-x}Cd_xO$ nanorods with controllable optical properties

Gao-Ren Li [a,*], Wen-Xia Zhao [b], Qiong Bu [a], Ye-Xiang Tong [a,*]

[a] MOE of Key Laboratory of Bioinorganic and Synthetic Chemistry, School of Chemistry and Chemical Engineering, Institute of Optoelectronic and Functional Composite Materials, Sun Yat-Sen University, Guangzhou 510275, China
[b] Instrumental Analysis and Research Center, Sun Yat-Sen University, Guangzhou 510275, China

ARTICLE INFO

Article history:
Received 6 September 2008
Received in revised form 16 November 2008
Accepted 18 November 2008
Available online 28 November 2008

Keywords:
Electrochemical deposition
Zn–Cd–O
Nanorod
Opitcal property
Semiconductor

ABSTRACT

Here we explored a novel and facile electrochemical route for the preparation of $Zn_{1-x}Cd_xO$ (x is atomic percentage of Cd) nanorods with controllable optical properties. The $Zn_{1-x}Cd_xO$ nanorods can be routinely obtained when the electrochemical deposition was carried out in solution of $Zn(NO_3)_2$ + $Cd(NO_3)_2$ + citric acid at −1.0 V (vs SCE). EDS results demonstrated that Cd, Zn, and O elements existed in the deposits, and ternary $Zn_{1-x}Cd_xO$ compounds were obtained. XRD results showed that $Zn_{1-x}Cd_xO$ nanorods were pure ZnO wurtzite structures. HRTEM and SAED analyses confirmed that $Zn_{1-x}Cd_xO$ nanorods were single-crystalline. The optical properties of $Zn_{1-x}Cd_xO$ nanorods were investigated in this paper.

1. Introduction

Among of group II–VI semiconductor materials, ZnO is one of the most attractive functional semiconductor materials for the fabrication of optoelectronic devices operating in the blue and ultraviolet region because of a direct wide band-gap of 3.37 eV and an exciton binding energy of 62 meV [1,2]. It is well known that the realization of band-gap engineering to create barrier layers and quantum wells in device heterostructures is an important step for the design of ZnO-based devices. CdO is an *n*-type degenerate semiconductor with a direct band-gap of 2.3 eV and an indirect band-gap of 1.36 eV [3]. The ternary $Zn_{1-x}Cd_xO$-alloy can allow a continuous expansion from 3.37 eV (band-gap of ZnO) to a narrower band-gap, i.e., into the visible spectral range, and their preparation have been widely reported [4].

The control over morphology and size of semiconductor materials represents a great challenge in realizing the design of novel functional devices. In recent years, one dimensional (1D) nanostructures, such as, nanowires, nanorods, nanobelts, and nanotubes, have been demonstrated to exhibit superior optical, electrical, catalytic, magnetic, and mechanical properties, indicating their potential applications as building blocks in microscaled devices. In this paper, we investigated an electrodeposition method by applying a negative potential to the substrate and demonstrated that $Zn_{1-x}Cd_xO$ nanorods can be successfully obtained. Electrochemical deposition allows mixing of the chemicals at atomic level thus reducing the possibility of undetectable impurity phases, [5] and it is a good candidate to solve the problem of the small thermodynamic solubility of CdO in ZnO [6] Furthermore, the electrochemical deposition presents a simple, quick and economical method for the preparation of $Zn_{1-x}Cd_xO$ nanorods.

2. Experimental

All the electrochemical experiments were carried out in a closed glass cell at 85 °C, in which a Cu plate, a graphite rod, and a saturated calomel electrode (SCE) served as the working electrode, counter electrode, and reference electrode, respectively. The Cu substrate was cleaned ultrasonically in 0.1 M HCl, distilled water, and acetone and then rinsed in distilled water again. The electrochemical deposition of $Zn_{1-x}Cd_xO$ films was carried out in solution of 0.1 mol dm^{-3} $Zn(NO_3)_2$ + 0.03 mol dm^{-3} $Cd(NO_3)_2$ + 0.05 mol dm^{-3} citric acid at the deposition potential of −1.0 V (vs SCE) for 60 min. The content of Cd in each sample was varied by changing the concentration of $Cd(NO_3)_2$ in deposition solution. After deposition, the sample was removed from the electrolyte, and rinsed first with acetone and then de-ionized water. X-ray energy dispersive spectroscopy (EDS) was used to determine the atomic percentage of Cd in the deposits. The surface morphology of the deposited $Zn_{1-x}Cd_xO$ nanorods were characterized by field emission scanning electron microscope (FE-SEM) and transmission

* Corresponding authors. Fax: +86 20 84112245 (G.-R. Li).
E-mail address: ligaoren@mail.sysu.edu.cn (G.-R. Li).

1388-2481/$ - see front matter
doi:10.1016/j.elecom.2008.11.024

electron microscopy (TEM). The powder X-ray diffractometry (XRD) and TEM were used to determine the crystal structure of $Zn_{1-x}Cd_xO$ nanorods. The absorption measurements were used to investigate the variations in optical transitions due to changes in x (Cd atomic percentage). Photoluminescence (PL) spectra were carried out by spectrofluorophotometer (RF-5301PC) at room temperature.

3. Results and discussion

SEM image of the prepared samples is shown in Fig. 1a, which shows the obtained sample is composed of nanorods. The average diameters of these nanorods are about 100 nm, and their lengths are about 1.5 μm. Fig. 1b shows transmission electron microscopy (TEM) image of the partial $Zn_{1-x}Cd_xO$ nanorod, which also shows the diameter of nanorod is about 100 nm. The high-resolution transmission electron microscopy (HRTEM) and selected area electron diffraction pattern (SAED) of $Zn_{1-x}Cd_xO$ nanorods were also measured, and the typical HRTEM image and SAED pattern were shown in the inset in Fig. 1b. The SAED pattern reveals the single-crystal wurtzite structure of the nanorod with a [0001] growth direction along the wire axis. The HRTEM image indicates a lattice spacing of 0.26 nm, corresponding to the (0001) planar spacing of ZnO in the wurtize phase. EDS measurements of $Zn_{1-x}Cd_xO$ nanorods were carried out at a number of locations throughout the films, and the representative EDS spectrum was shown in Fig. 1c. The composition analysis showed that Cd percentage in $Zn_{1-x}Cd_xO$ nanoparticle aggregate was 8 at.%, Zn percentage was 92 at.% (The copper peaks come form the substrate).

In this study, nitrate ions (NO_3^-) is firstly elecro-reduced to form hydroxyl ions (OH^-) via Eq. (1) [7] The produced OH^- will react with Zn^{2+} to form $[Zn(OH)_4]^{2-}$ and then form ZnO via Eq. (2) as the increase of pH near the working electrode. At the samt time, Cd^{2+} will also react with the produced OH^- to form $Cd(OH)_2$ and then form CdO via Eq. (3). As we all know, the electrochemical deposition can allow mixing of the chemicals at atomic level, so the produced ZnO and CdO will uniformly mix, and accordingly the $Zn_{1-x}Cd_xO$ alloys were prepared.

$$NO_3^- + H_2O + 2e \rightarrow NO_2^- + 2OH^- \quad (1)$$

$$4OH^- + Zn^{2+} \rightarrow [Zn(OH)_4]^{2-} \rightarrow ZnO + H_2O \quad (2)$$

$$2OH^- + Cd^{2+} \rightarrow Cd(OH)_2 \rightarrow CdO + H_2O \quad (3)$$

$$(1-x)ZnO + xCdO \rightarrow Zn_{1-x}Cd_xO \quad (4)$$

Fig. 2 shows XRD spectra of the $Zn_{1-x}Cd_xO$ ($0 \leqslant x \leqslant 0.15$) alloys in the range of $2\theta = 10$–$80°$. For all the samples, three peaks corresponding to (100), (002), and (101) of wurtzite structured ZnO (hexagonal phase, space group $P63mc$) appeared (JCPDS 36-1451). The peaks marked with Cu (111) and (200) correspond to Cu substrate. No any relational Cd or CdO crystalline forms are detected, which shows no phase separation existed in $Zn_{1-x}Cd_xO$ nanorods. This is accordant with the results of HRTEM and SAED. The prepared $Zn_{1-x}Cd_xO$ films exhibiting hexagonal wurtzite structures similar to ZnO because Zn has a larger chemical activity than Cd, and is easier to form crystal frames [8,9]. From the intensities of the XRD peaks, it can be observed that the parameters increase with increasing Cd contents in the $Zn_{1-x}Cd_xO$ films. From $x = 0.05$ to $x = 0.15$, the half weight of full maximums (FWHM) of the (002) peaks related to the hexagonal $Zn_{1-x}Cd_xO$ phases also increase with increasing Cd contents as shown in Fig. 2. According the Scherrer's relation, it is easily known that the average size of the crystal grains in the deposits decrease with increasing Cd contents. In addition, it should be noted that a lower angle shift was observed in XRD spectra of $Zn_{1-x}Cd_xO$ deposits in Fig. 2 with increasing Cd contents. It is undoubted that the substitutions of

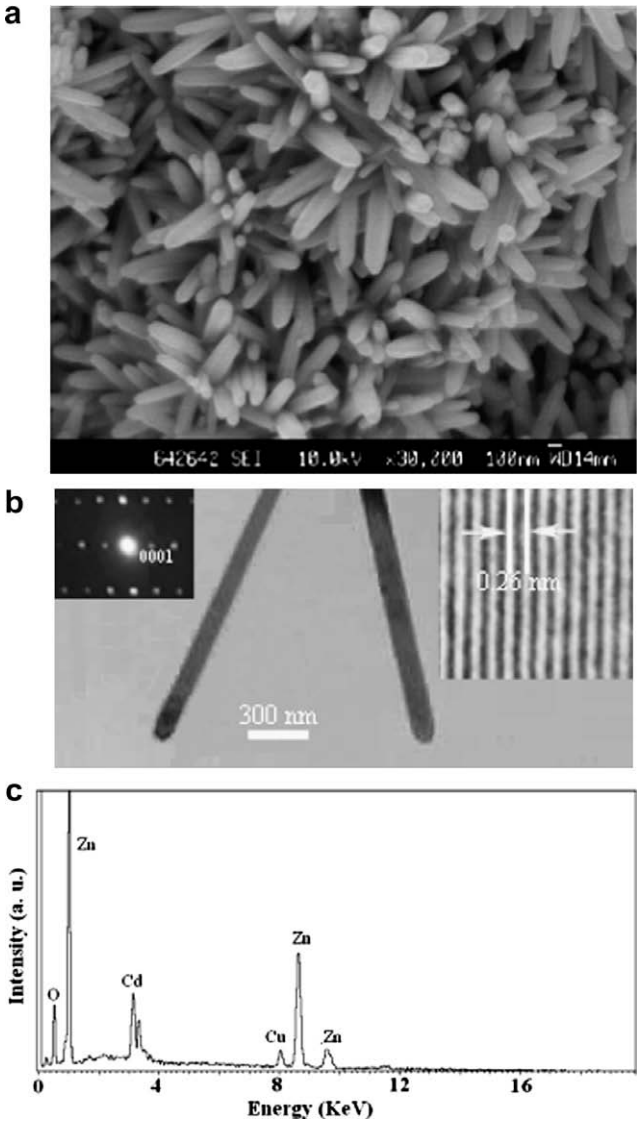

Fig. 1. (a) SEM image of $Zn_{1-x}Cd_xO$ nanorods prepared in solution of 0.1 mol dm^{-3} $Zn(NO_3)_2$ + 0.03 mol dm^{-3} $Cd(NO_3)_2$ + 0.1 mol dm^{-3} citric acid at −1.0 V (vs SCE). (b) TEM, SEAD (left inset), and HRTEM (right inset); (c) EDS pattern.

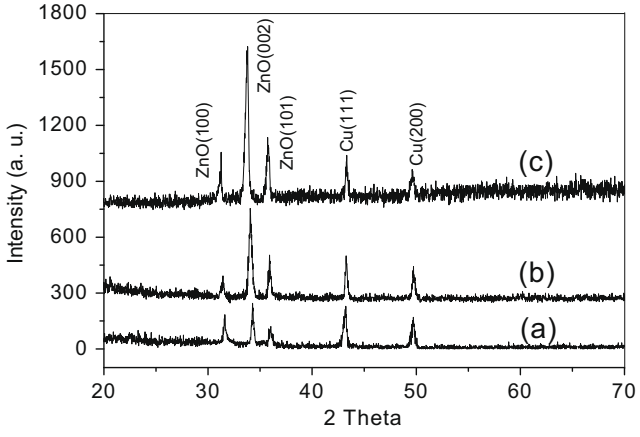

Fig. 2. X-ray diffraction patterns of the prepared $Zn_{1-x}Cd_xO$ nanorods with different Cd contents (a): 5 at.%; (b): 9 at.%; and (c): 15 at.%.

Zn by Cd take place on the equivalent crystallographic positions of Zn in hexagonal wurtzite structures. As the ionic radius of Cd (0.97 Å) is larger than that of Zn (0.74 Å), so the cell volume will be increased when Cd enters into ZnO lattices, which will cause the shifts of ZnO (100), (002), and (101) peaks to lower angles.

The optical transmittance measurements of $Zn_{1-x}Cd_xO$ films with various Cd contents were carried out, and the transmittance spectra were shown in Fig. 3a. Good transmittances in the visible region were observed for all the samples. However, with increasing Cd content in deposits, the poorer transmittance is observed. This can be explained as follows. When more Cd elements were incorporated into ZnO, the band-gap of $Zn_{1-x}Cd_xO$ will become narrower, and more oxygen vacancies and cadmium, zinc interstices will be produced, which will lead to higher carrier concentration and accordingly will damage the optical transmittance [10]. When the Cd content in deposits was increased to 15 at.%, the apparent oscillations in the transmittance spectra are observed in Fig. 3a, and this can be attributed to the interference fringes [11]. The interference fringes come from the superposition of two or more waves that originate from the same point on the same source. In addition, it should be noted that the absorption edge for $Zn_{1-x}Cd_xO$ films with 15 at.% Cd shows a rather slow decay, which can be attributed to a band-tail absorption caused by the large carrier concentration [12].

According to the data for the transmittance spectra, the absorption coefficients (α) of $Zn_{1-x}Cd_xO$ can be estimated by using the following equation [13]:

$$\alpha = [2.303 \times \log(1/T)]/d \quad (5)$$

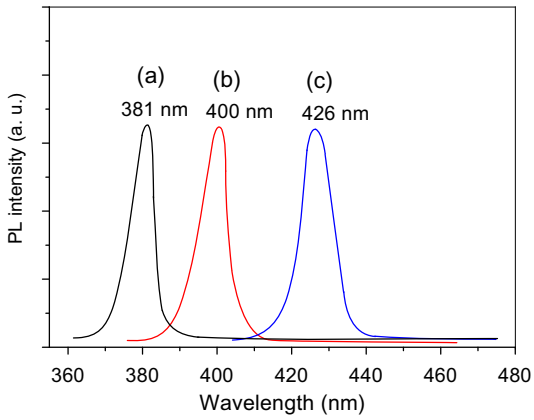

Fig. 4. PL spectra of $Zn_{1-x}Cd_xO$ nanorods with different Cd contents. (a) 5 at.%; (b) 9 at.%; (c) 15 at.%.

where T represents for the transmittance and d for the film thickness. Then the optical band-gaps (E_g) of $Zn_{1-x}Cd_xO$ can be estimated by using the following equation [14]:

$$\alpha h\upsilon = C(h\upsilon - E_g)^n \quad (6)$$

where α is the absorption coefficient, $h\upsilon$ is photon energy, C is the constant. The plot curves $(\alpha h\nu)^2$ vs. $h\nu$ was shown in Fig. 3b. The optical band-gaps of the $Zn_{1-x}Cd_xO$ alloys with 0, 5, 9, and 15 at.% can be estimated as 3.37, 3.25, 3.10, and 2.91 eV, respectively. These results demonstrate the band-gap energies of the ternary $Zn_{1-x}Cd_xO$

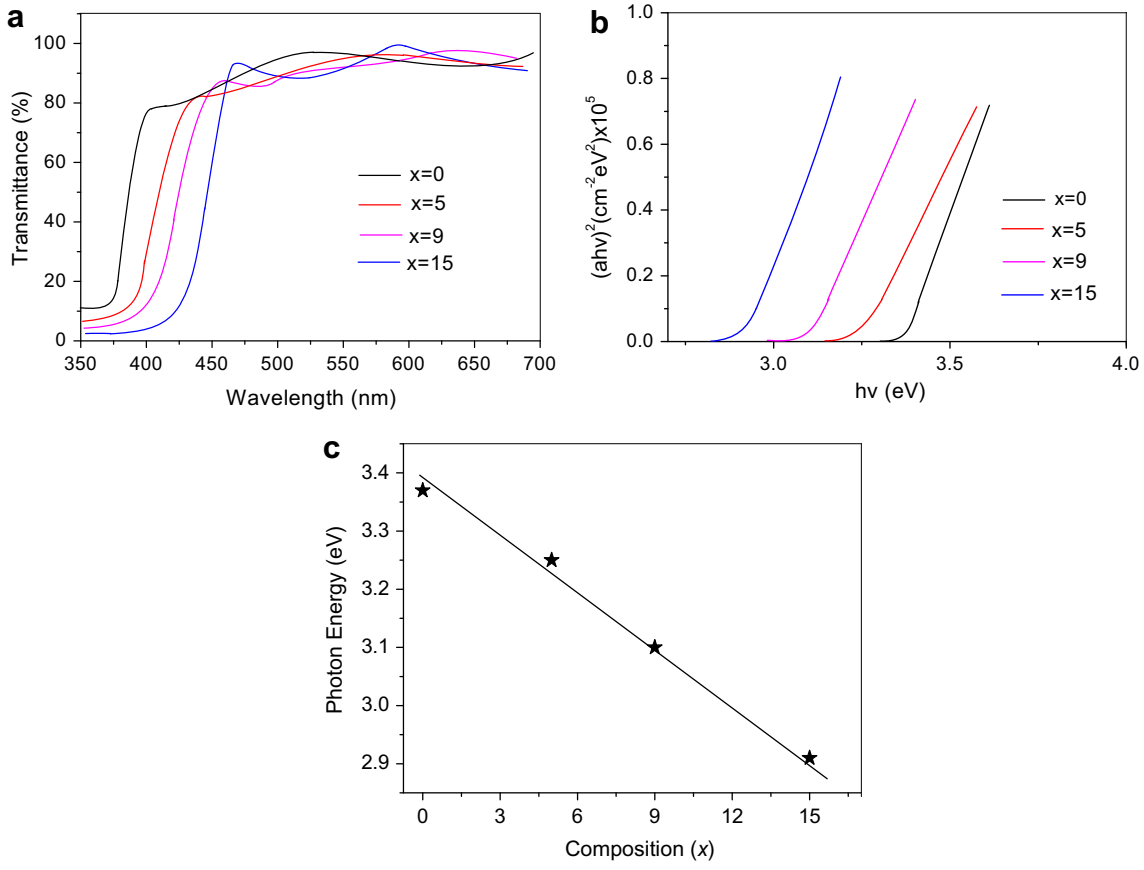

Fig. 3. Optical transmittance spectra of $Zn_{1-x}Cd_xO$ ($0 \leqslant x \leqslant 0.15$) nanorods; (b) Plots of $(\alpha h\nu)^2$ vs. hν as a function of Cd contents x; (c) The energy gaps of $Zn_{1-x}Cd_xO$ as a function of composition x.

alloys decrease with the Cd content increasing. The energy gaps of the $Zn_{1-x}Cd_xO$ nanorods as a function of composition x were plotted in Fig. 3c.

The normalized photoluminescence (PL) spectra of the $Zn_{1-x}Cd_xO$ nanorods with Cd content increasing were shown in Fig. 4. These PL spectra have been labeled with wavelength of the maximum intensity for each sample. All the PL data have been corrected for the spectral response of our detection system. It can be clearly observed that the near-band-gap emission of $Zn_{1-x}Cd_xO$ nanorods changed from 381 nm to 426 nm with the Cd content increasing. Furthermore, the position of the near-band-gap PL maximum can be continuously changed anywhere within 381 nm to 426 nm. The redshift of UV emission peak was attributed to the narrowing of E_g, which was reduced from 3.25 to 2.91 eV with Cd content increasing from 5 to 15 at.%.

4. Conclusions

Here we showed the electrodeposition of $Zn_{1-x}Cd_xO$ nanorods with controllable optical properties. HRTEM and SAED analyses confirmed that $Zn_{1-x}Cd_xO$ nanorods were single-crystalline. XRD results showed that $Zn_{1-x}Cd_xO$ nanorods were pure ZnO wurtzite structures. The band-gaps of $Zn_{1-x}Cd_xO$ alloys can be well adjusted by changing the composition. For $x = 0.05$, 0.09, 0.15, the band-gaps of the $Zn_{1-x}Cd_xO$ alloys were estimated as 3.25, 3.10, and 2.91 eV, respectively. Photoluminescence spectra show that the near-band-edge energy of $Zn_{1-x}Cd_xO$ nanorods has a red-shift with Cd content increasing.

Acknowledgements

This work was supported by the Natural Science Foundations of China (Grant Nos. 20603048 and 20873184).

References

[1] V.E. Henrich, P.A. Cox, The Surface Science of Metal Oxides, Cambridge University Press, Cambridge, 1994.
[2] H. Cao, J.Y. Xu, D.Z. Zhang, S. -H. Chang, S.T. Ho, E.W. Seelig, X. Liu, R.P.H. Chang, Phys. Rev. Lett. 84 (2000) 5584.
[3] I.D. Makuta, S.K. Poznyak, A.I. Kulak, E.A. Streltsov, Phys. Status Solidi A 111 (1989) 193–199.
[4] C.X. Shan, Z. Liu, Z.Z. Zhang, D.Z. Shen, S.K. Hark, J. Phys. Chem. B 110 (2006) 11176–11179.
[5] Y.-J. Li, C.-Y. Wang, M.-Y. Lu, K.-M. Li, L.-J. Chen, Cryst. Growth Des. 8 (2008) 2598–2602.
[6] F. Bertram, S. Giemsch, D. Forster, J. Christen, R. Kling, C. Kirchner, A. Waag, Appl. Phys. Lett. 88 (2006) 061915.
[7] L. Xu, Q. Chen, D. Xu, J. Phys. Chem. C 111 (2007) 11560–11565.
[8] D.W. Ma, Z.Z. Ye, L.L. Chen, Phys. Status Solidi A 201 (2004) 2929–2933.
[9] O. Vigil, L. Vaollant, F. Cruz, G. Santana, A. Moroles-Acevedo, G. Contreras-Puente, Thin Solid Films 361 (2000) 53.
[10] T.K. Subramanyam, B. Srinivasulu Naidu, S. Uthanna, Appl. Surf. Sci. 529 (2001) 169–170.
[11] J. Hu, R.G. Gordon, J. Appl. Phys. 71 (1992) 880.
[12] Y.Y. Zhang, Semiconductors Optoelectronics, vol. 52, Shanghai Science and Technology Publishing Company, Shanghai, 1987 (in Chinese).
[13] D.M. Carballeda-Galicia, R. Castanedo-Pérez, O. Jiménez-Sandoval, S. Jiménez-Sandoval, G. Torres- Delgado, C.I. Zúñiga-Romero, Thin Solid Films 371 (2000) 105.
[14] E. Ziegler, A. Heinrich, H. Oppermann, G. Stover, Phys. Status Solidi A 66 (1981) 635.